Muscle Architecture Measurements from DT-MRI Fiber Tracking: Tract Smoothing and Voxel Size Considerations

B. M. Damon[1,2]

[1]Radiology and Radiological Sciences, Vanderbilt University, Nashville, TN, United States, [2]Institute of Imaging Science, Vanderbilt University, Nashville, TN, United States

Introduction

Muscle architectural properties such as fiber length, pennation angle, and curvature influence force production, shortening velocity, and the development of intramuscular pressure during contraction. Diffusion-tensor MRI-based muscle fiber tracking can reproducibly quantify human muscle architecture in 3D (1,2), but the estimation of the muscle diffusion tensor (**D**) is noise-sensitive (3). Fiber tract smoothing and optimizing the voxel dimension-influenced tradeoff between signal-to-noise ratio (S/N) and spatial resolution may help to reduce the effects of noise on the calculated architectural parameters. Thus the purposes of this study were: 1) to investigate the potential for polynomial fitting of the fiber tracts to reduce the effects of noise on the architectural parameters and 2) to investigate the sensitivity of the architectural parameters to voxel size and aspect ratio (AR=slice thickness/in-plane dimension).

Methods

Tissue Model All analyses were performed in Matlab. To create a condition of known fascicle length, pennation angle, and curvature, a fascicle from a 2D ultrasound (US) image of a muscle was digitized (Fig. 2 of Ref. (4)). The foot-head and anterior-posterior directions in the US image were defined as the Z and Y axes, respectively. To generate a smooth curve describing the fascicle's spatial properties (the "original fascicle"), the Y values were fitted to a 3rd order polynomial as a function of Z position; the polynomial was solved for Z values incrementing from the minimum to maximum Z value in 0.1 mm steps.

Synthetic Images Four sets of diffusion-weighted images were generated. The images had isotropic (ISO) resolution or AR=3.4, voxel volume=8 or 27 mm^3, and low or high S/N (Table 1). Within image slices, the first eigenvector (ε_1) of **D** was defined as the local tangent to the smoothed fascicle; ε_2 was the in-plane normal to ε_1; and ε_3 was defined as $\varepsilon_1 \times \varepsilon_2$. The eigenvalues of **D** were assumed to be 2.0, 1.6, and 1.4×10^{-3} mm^2/s (2,3). Image signal intensities were calculated for a T_2-weighted image and diffusion-weighted images (15 directions), assuming full longitudinal magnetization and substituting T_2=35 ms, TE=45 ms, and b=0 or 500 s/mm^2 into standard signal equations. Rician noise was added to each set of images to create the desired S/N.

Table 1. Properties of the image sets.

Condition	Resolution (mm)	S/N
ISO-8-Low	2×2×2	45
ISO-8-High	2×2×2	145
AR3.4-8	1.33×1.33×4.88	45
ISO-27	3×3×3	145

Image Analysis In each voxel, **D** was estimated using weighted least squares and diagonalized; λ_1, λ_2, and λ_3 were magnitude-sorted. A single fiber tract was generated from slice #1 by following the direction indicated by ε_1 and terminating the tracking procedure if the fiber tract moved out of bounds, if the fractional anisotropy was <0.1 or >0.4, or if the angle formed by two successive fiber tracking steps was >45°. The X, Y, and Z positions of the raw fiber tract were fitted to 2nd order polynomials as functions of point number. For each point along the original fascicle and the raw and fitted fiber tracts, the pennation angle was calculated as the arccosine of the dot product of the local tangent to the fiber tract and a unit vector in the +Z direction and curvature was calculated using the Frenet-Serret formulae. These procedures were repeated using 1000 independent noise realizations per image set. Fiber tracts with L_{fit}>90% of the length of the original fascicle were used for further analysis. The mean and 95% confidence interval (95%CI) were calculated for the pennation angle and curvature, at 10% distance intervals along the fitted tract.

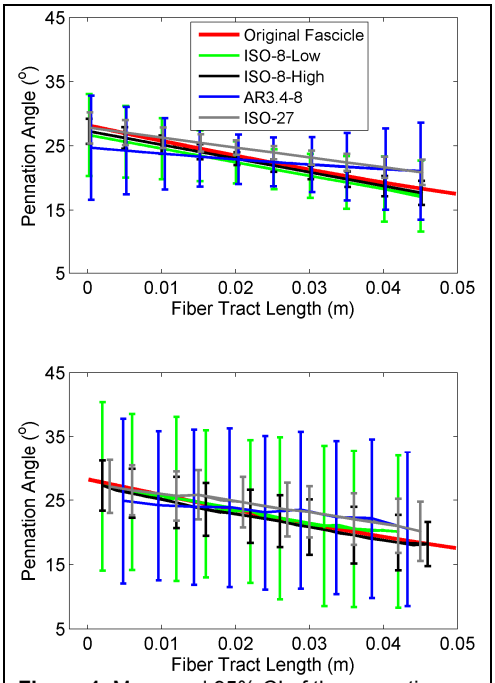

Figure 1. Mean and 95% CI of the pennation angle for the fitted (top panel) and raw (lower panel) tracts; see legend for data identity.

Results and Discussion

Pennation Angle Figure 1 shows the mean and 95%CI for pennation angle for the fitted fiber tracts and the raw fiber tracts. Also shown in each plot are the known pennation angle data for the original fascicle. For all image sets with 8 mm^3 voxels, pennation angle was accurately estimated (*i.e.,* the 95%CI's of the fitted tracts contained the values of pennation angle for the original fascicle). All image sets with high S/N had higher precision (smaller 95%CI's) than the image sets with low S/N. Similar precision trends were also noted for the raw fiber tracts. Also, in all cases, the 95%CI's for mean pennation angle the raw fiber tracts contained the pennation values of the original fascicle.

Curvature Figure 2 shows the mean and 95%CI's for the curvature values of the fitted fiber tracts from the four image sets as well as the curvature data for the original fascicle. Because of the point-wise effect of noise, the curvature values for the raw fiber tracts were unreasonably high (>100 m^{-1}) and are not shown. At each position measured along the tract, the 95%CI's for mean curvature of each of the image sets that had a voxel volume of 8 mm^3 contained the known curvature values. In the 27 mm^3 voxel volume images, curvature was underestimated, especially in the initial portion of the fiber tract. For the ISO-8 image sets, the precision of the curvature measurements improved with S/N.

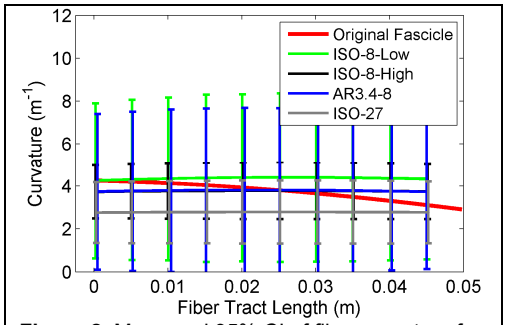

Figure 2. Mean and 95% CI of fiber curvature for the raw and fitted tracts; see legend for data identity.

Conclusions

Smoothing DT-MRI muscle fiber tracts improves the accuracy and precision of muscle fiber curvature measurements and the precision of pennation angle measurements. The accuracy and precision of the curvature and pennation angle measurements for the smoothed tracts were unaffected by voxel aspect ratio. Rather, the accuracy was most affected by voxel size and the precision was most affected by S/N.

References

1. Lansdown DA, et al. *J Appl Physiol* 2007; **103**:673. **2.** Heemskerk AM, et al. *NMR Biomed* 2010; **23**:294. **3.** Damon BM. *Magn Reson Med* 2008; **60**: 934. **4.** Muramatsu T, et al. *J Appl Physiol* 2002; **92**:129.

Acknowledgements: NIH/NIAMS AR050101